CRYSTAL FIELD ASPECTS OF THE VIBRATIONAL SPECTRA OF METAL COMPLEXES

DAVID A. THORNTON

Department of Inorganic Chemistry, University of Cape Town, Rondebosch 7700 (South Africa)

(Received 30 June 1983)

CONTENTS

A. INTRODUCTION

Prior to 1967, when the author and his colleagues began a study of crystal field aspects of the vibrational spectra of metal complexes, there had been only occasional observations in the literature on the characteristics of metal–ligand frequencies of a series of complexes $[ML_6]^{n+}$ in which L and n are constant and M varies through a transition series. These comments had been limited to observing that, for first transition series metal ions, the frequencies vary with $3d$-orbital population according to the Irving–Williams [1] stability sequence. This sequence, although originally described in terms of ionization potentials, has its origins in crystal field theory. It therefore seemed opportune for the author and his colleagues to make a detailed investigation of the relationship between metal–ligand stretching frequency ($\nu M-L$) and crystal field stabilization energy (CFSE) which had, for instance, been hinted at by Sacconi and Sabatini [2,3] and Adams et al. [4].

Although it is sometimes necessary to use the more elaborate molecular

orbital theory to account for the bonding in metal complexes (especially where π-bonding is important), most situations are adequately accounted for by the simpler crystal field (CF) theory and the qualitative aspects of this theory will be used throughout this discussion.

In CF theory we consider what happens to the energies of the d-orbitals of a transition metal ion during complex formation but first we should consider the total energy changes occurring on metal ion complexation (Fig. 1). The principal driving force behind complex formation is the electrostatic attraction between the metal cation and the coordinated anions (or the negative ends of the ligand dipoles). There follows the repulsion suffered between the electrons in the s-, p- and d-orbitals of the metal ion and the ligand electrons. This leads to an increase in the energies of the s-, p- and d-orbitals. Figure 2 shows the overlap between these orbitals and the ligand orbitals in the formation of an octahedral complex from a metal ion and six equivalent ligands

$$M^{n+} + 6L \rightarrow [ML_6]^{n+} \tag{1}$$

Since the three p-orbitals are directed along the axes of ligand approach (for convenience, we define these axes as the x-, y- and z-axes of Cartesian coordinates with the metal ion at the origin), each p-orbital is equally raised in energy. The d-orbitals may be classified as those which lie along the axes (the $d_{x^2-y^2}$ and d_{z^2} orbitals, collectively known as the e_g orbitals) and those which lie between the axes (the d_{xy}, d_{yz} and d_{xz} orbitals, collectively known as the t_{2g} orbitals). The e_g orbitals suffer more repulsion than the t_{2g} orbitals on ligand approach so that the degeneracy of the five d-orbitals is removed as indicated in the last stage of Fig. 1.

The result of CF splitting is to stabilize the complex relative to the situation which obtains in the absence of CF splitting. Although the energy change resulting from CF splitting is a very small part of the total energy decrease on complex formation, the variation in many physical properties across the first transition series may be interpreted in terms of the stabiliza-
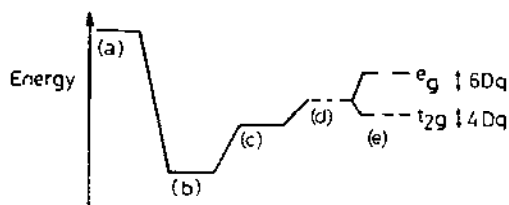

Fig. 1. Energy changes on octahedral complexation: (a) free ion level; (b) metal–ligand attraction; (c) destabilization of s- and p-orbital electrons; (d) destabilization of d-orbital electrons; (e) crystal field splitting.
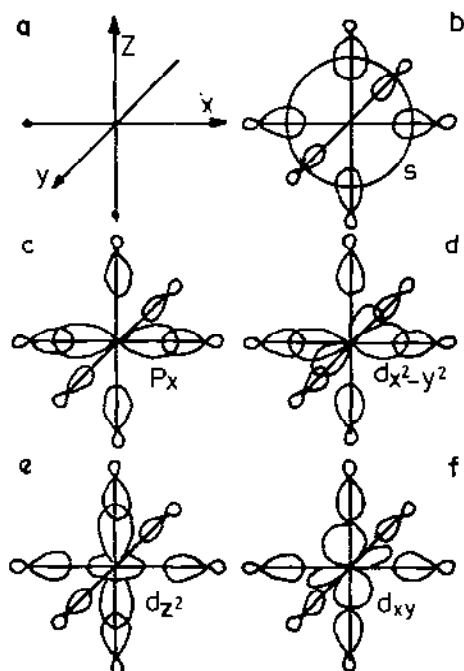
Fig. 2. Interaction of representative s-, p- and d-orbitals of a transition metal ion with six ligands in the formation of an octahedral complex: (a) the octahedral system of axes; (b) interaction of an s-orbital with six ligand orbitals; (c) interaction of a p_x-orbital with ligand orbitals (similar overlap occurs with the p_y and p_z orbitals); (d, e) interaction of the two e_g d-orbitals with ligand orbitals; (f) interaction of one of the three t_{2g} d-orbitals with ligand orbitals (note the absence of orbital overlap).

tion resulting solely from CF splitting. This is because the other energy changes depicted in Fig. 1 are either approximately constant or vary smoothly through the series (given constant metal ion charge and common structure) whereas the CF stabilization varies irregularly through the series.

A measure of the stabilization resulting from CF splitting is provided by the CF stabilization energy (CFSE), which is a function of d-orbital population and the magnitude of the CF splitting, $10Dq$:

$$\text{CFSE} = -(4n_t - 6n_e)Dq + P \tag{2}$$

for octahedral complexes, where n_t and n_e are the occupation numbers of the t_{2g} and e_g orbitals, respectively, and P (the pairing energy relevant only for low-spin ions) is the energy required to force electrons to pair up in a single orbital. In the examples cited in this paper, P is finite only for spin-paired Co^{3+}, which, among first transition metal ions, is the only commonly spin-paired ion.

Figure 3 shows how CFSE varies with $3d$-orbital population to yield a double-humped curve. Minima occur at $3d^0$, $3d^{10}$, and spin-free $3d^5$ (which have zero CFSE) while maxima occur at $3d^3$ and $3d^8$, which have maximum CFSE in octahedral coordination.

Equation 2 yields CFSE values in terms of Dq, which is not constant through the series. Since our discussion will relate largely to octahedral complexes of general formula $[ML_6]^{n+}$, where L and n are constant while M varies, it is somewhat more precise to use a different form of eqn. (2):
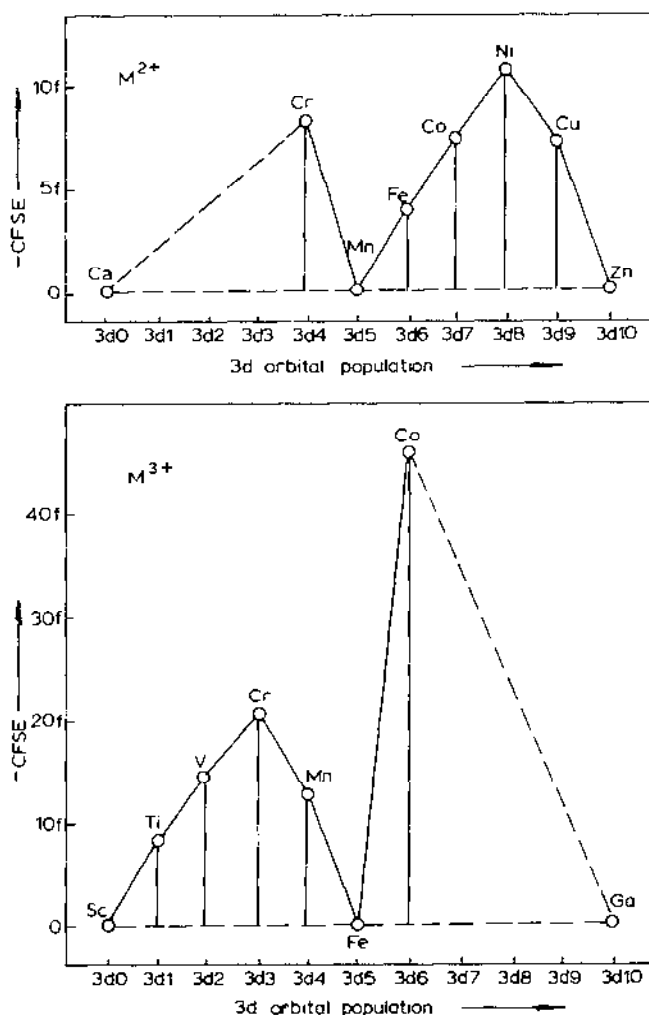
$$CFSE = -(0.4n_t - 0.6n_e)fg + P \tag{3}$$

Fig. 3. Variation of CFSE (in units of f) with $3d$-orbital population.

where

$$10Dq = fg \tag{4}$$

Equation 4 represents the factorization of $10Dq$ into a ligand component (f) and a metal ion component (g). The ligand parameter, f, provides an index of the CF splitting power of the ligand (that is, its position in the spectrochemical series) while the metal ion parameter, g, is the 10 Dq value of the complex of the metal ion with 6 H_2O (for which f is unity). Thus, if we are to compare the CFSEs of a series of complexes $[ML_6]^{n+}$ (L and n constant, M variable), then we may use the known values of g for the various M^{n+} ions to calculate the CFSEs from eqn. (3) in terms of the constant ligand parameter, f. If the value of f is available, absolute values of the CFSEs, usually expressed in kiloKayser (kK; 1 kK = 1000 cm^{-1}) may be obtained. In Fig. 3, the CFSEs are plotted in units of f and the relationship shown will apply to any series of octahedral complexes, $[ML_6]^{n+}$.

The information to be derived from Fig. 3 is that (ignoring all other factors which may influence complex stability) $3d^3$ and $3d^8$ ions will be most stabilized by CF splitting for M^{2+} complexes. In practice, $3d^4$ is the real first maximum, since the $3d^3$ M^{2+} ion (V^{2+}) is unstable and, frequently, $3d^9$ (Cu^{3+}) is the real second maximum, since this configuration is additionally stabilized by Jahn–Teller distortion. For M^{3+} ions, the second real peak is usually at $3d^6$, since this ion (Co^{3+}) is usually spin-paired and the $3d^8$ ion (Cu^{3+}) is unstable. Nevertheless, the double-humped shape remains.

B. METAL–LIGAND STRETCHING FREQUENCIES

For a diatomic molecule, the relationship between the bond stretching frequency (ν), the force constant (f) and the reduced mass (μ) is given by

$$\nu = k(f/\mu)^{1/2} \tag{5}$$

where k is a constant.

If we now consider each M–L bond in a series of complexes $[ML_6]^{n+}$ (L and n constant while M varies through the first transition series) to behave as a diatomic molecule, then eqn. (5) will apply to the M–L bonds. As the $3d$-orbital population of M increases, the force constant of each M–L bond will vary in sympathy with CFSE (that is, irregularly) while μ will show a relatively smooth increase, which induces a regular decrease in ν. At the same time the decrease in ionic radius through the series will increase f and hence ν.

The infrared spectra (Fig. 4) of the pyridine N-oxide (pyO) complexes of the metal(II) perchlorates, $[M(pyO)_6](ClO_4)_2$ (M = Mn, Fe, Co, Ni, Cu, Zn) enable the validity of these arguments to be tested [5]. The solid bands in

Fig. 4 are the metal–oxygen stretching bands (νM–O) assigned on the basis of their significant sensitivity to deuteration of pyO. Figure 5 shows a plot of νM–O against $3d$-orbital population. The interpolation line is considered to represent the frequencies (ν_0) which would have been realized in the absence of CF effects. Hence ($\nu - \nu_0$) represents the contribution of CFSE to νM–O. There is good qualitative agreement between ($\nu - \nu_0$) and CFSE (Table 1). The positive slope of the interpolation line is attributed to the fact that the ionic contraction through the series (tending to increase νM–O) overrides the mass effect (tending to reduce νM–O).

The unique character of the spectrum of the 6-coordinate Cu^{2+} complex deserves special mention. The complexes of the other M^{2+} ions have O_h site symmetry and one νM–O band is observed in accordance with the selection rules. The Cu^{2+} complex is tetragonally distorted (Jahn–Teller distortion of the 4 short-, 2 long-bond type). Tetragonal D_{4h} symmetry requires two infrared-active νM–O bands, and two are observed. The νM–O band of higher frequency corresponds with the short (strong) Cu–O bonds while the lower frequency component arises from the long (weak) Cu–O bonds. It is
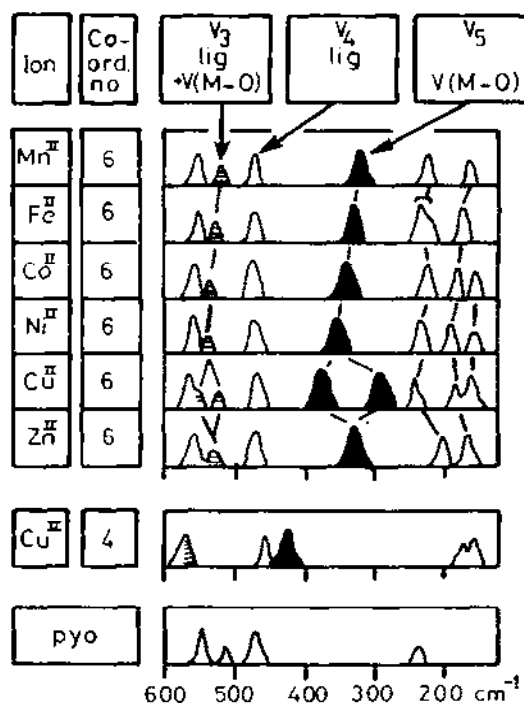

Fig. 4. Infrared spectra of the pyridine N-oxide (pyO) complexes $[M(pyO)_6](ClO_4)_2$ (M = Mn, Fe, Co, Ni, Cu, Zn) and $[Cu(pyO)_4](ClO_4)_2$. Solid bands: νM–O; shaded bands: coupled νM–O.

TABLE 1

$\nu M-O$, $(\nu - \nu_0)$ and CFSE data for the complexes $[M(pyO)_6](ClO_4)_2$

Parameter	Mn $3d^5$	Fe $3d^6$	Co $3d^7$	Ni $3d^8$	Cu $3d^9$	Zn $3d^{10}$
$\nu M-O$ (cm^{-1})	314	322	333	345	372, 284	323
$(\nu - \nu_0)$ (cm^{-1})	0	6	15	26	7 [a]	0
$-CFSE_{theor}$ (kK) [b]	0	4	7	10	6	0

[a] Based on mean value of two $\nu Cu-O$ bands.
[b] From CFSE $= -(0.4n_t - 0.6n_e)fg$ (f for $(pyO)_6 = 0.90$).

the mean of these two frequencies which is plotted in Fig. 5. Splitting of $\nu M-L$ bands is a very sensitive index of distortion to lower symmetry.

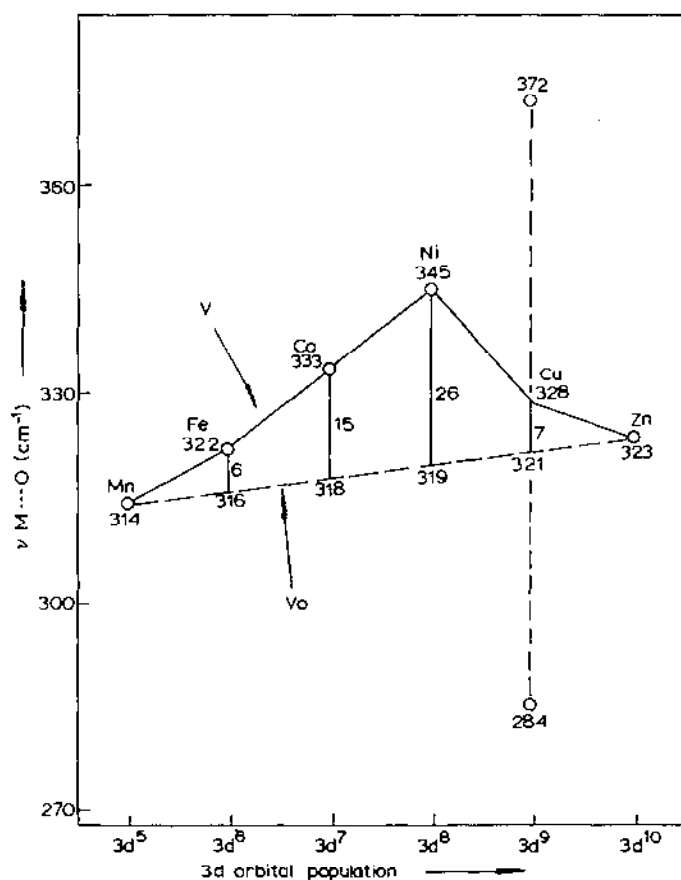Besides the 6-coordinate tetragonal Cu^{2+} complex mentioned above, it is

Fig. 5. Variation of metal–oxygen stretching frequencies ($\nu M-O$) of the complexes $[M(pyO)_6](ClO_4)_2$ with $3d$-orbital population.

possible to synthesize a 4-coordinate Cu^{2+} complex, $[Cu(pyO)_4](ClO_4)_2$. For the square-planar D_{4h} site symmetry of this complex, one $\nu M-O$ band is expected and one is observed. This band is at a considerably higher frequency than the $\nu M-O$ bands of the 6-coordinate Cu^{2+} complex (Fig. 4). This feature is associated with the change of coordination number. The bonding capacity of the Cu^{2+} ion is distributed over fewer bonds in the 4-coordinate complex, so the electron density (and hence the force constant of each Cu–O bond) is higher.

C. METAL TROPOLONATE SPECTRA

The most comprehensive set of infrared data obtained by the author and his colleagues [6–11] refers to the metal tropolonates (Fig. 6). Except for Cu(II), which shows its usual preference for square planar coordination, the metal(II) and metal(III) ions of the first transition series yield octahedral tropolonate complexes which are formulated $[MT_2]_n$ and $[MT_3]$, respectively (T = tropolonate anion). In the metal(II) complexes, 6-coordination is achieved by polymerization involving bridging tropolonate units, the well-known structural analogy being the metal(II) acetylacetonate complexes.

Figure 7 depicts the spectra of all the preparatively accessible tropolonates of the first transition series ions. ^{18}O-labelling [12] of the Cu(II) complex reveals that all five bands within the range 720–400 cm^{-1} are shifted towards lower frequencies by the mass effect of the heavier isotope. The two shaded bands in Fig. 7 (spectrum of Cu(II) complex) exhibit the maximum ^{18}O-induced shifts which are sufficiently similar in magnitude for both bands to be considered as principal $\nu M-O$ bands. The corresponding bands (also shaded) in the spectra of the remaining complexes are readily identified. The higher frequency component of this band pair yields the correlation with $3d$-orbital population shown in Fig. 8. The striking similarity of the correlation with that of Fig. 3, in which CFSE is plotted against $3d$-orbital population, suggests that the frequency variation has its origin in crystal field effects (the unique character of the Cu(II) and Mn(III) complexes will be referred to separately).

The tropolonates of the ions with $3d^0$, spin-free $3d^5$ and $3d^{10}$ configurations are not stabilized by the crystal field. Their spectra may be considered
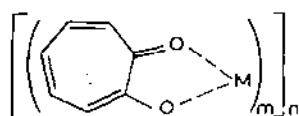
M = M(III): $m = 3$, $n = 1$
M = M(II) ≠ Cu(II): $m = 3$, $n > 1$
M = Cu(II): $m = 2$, $n = 1$

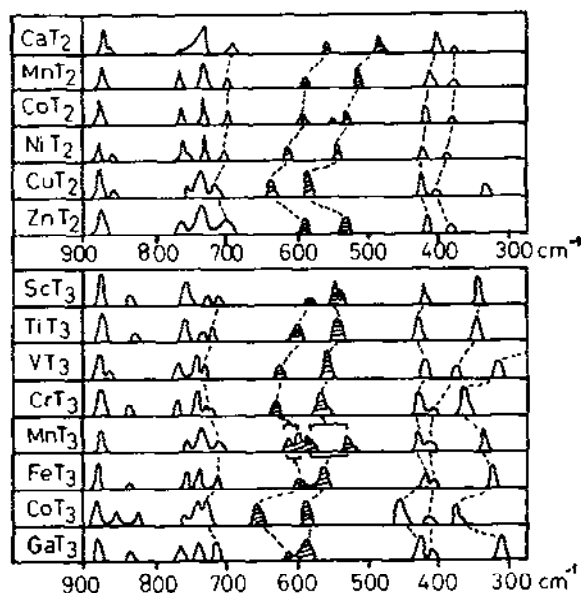Fig. 6. Formulae of the metal tropolonates.

Fig. 7. Infrared spectra of metal tropolonates. The principal νM–O bands are shaded.
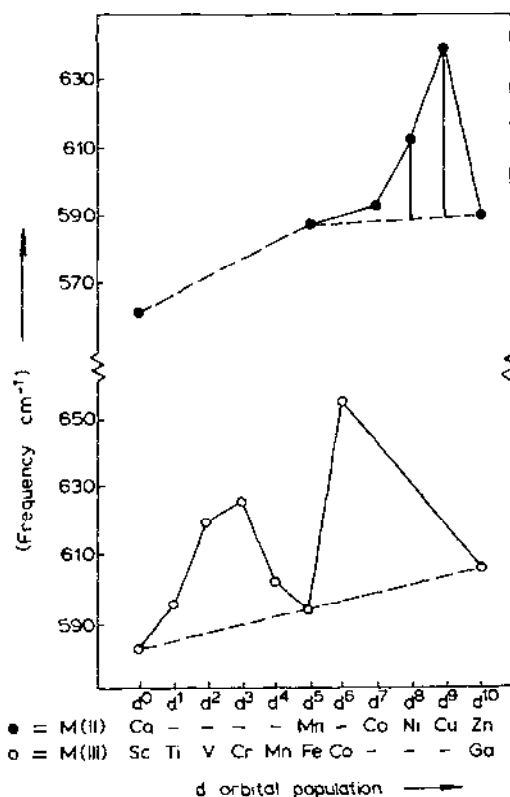

Fig. 8. Relationship between νM–O and $3d$-orbital population for metal tropolonates. The dashed lines represent ν_0 and the vertical lines represent $(\nu - \nu_0)$.

as reference spectra from which crystal field effects are absent. Hence, the interpolation line (the dashed line in Fig. 8) drawn through the points for these ions represents the frequencies (ν_0) which would have been realized for the complexes of all other ions in the absence of crystal field stabilization. The difference ($\nu - \nu_0$) between the observed and interpolated frequencies therefore represents that part of νM–L contributed by the CFSE. There is clearly (Table 2) an excellent correlation between ($\nu - \nu_0$) and CFSE with the exceptions to be noted in the following two paragraphs.

The tropolonates of Cu(II) and Mn(III) are unique in comprising the only two ions which are expected to give rise to strong Jahn–Teller distortion. The CFSE data in Table 2 are based on the assumption of octahedral coordination. However, the crystal structure of copper tropolonate [13,14] shows that the coordination is very nearly square planar. The effect of 4-coordination on νM–L may be discussed from two points of view. Either we may conclude that the bonding capacity of the metal ion is distributed over fewer M–O bonds than in the remaining 6-coordinate complexes (with a consequent increase in the force constant in the Cu–O bonds), or we may consider square planar structure as being an extreme example of tetragonal distortion (and hence giving rise to large Jahn–Teller stabilization). Either argument leads to the expectation of an exceptionally high value of νCu–O. It is therefore not surprising to find that the νM–O values of the metal(II)

TABLE 2

Magnetic moment, CFSE and infrared data on metal tropolonate complexes

Complex	Configu- ration	μeff (B.M.)	g(kK)	−CFSE (kK)	νM–O [a] (cm^{-1})	νM–O [a] (cm^{-1})
$[CaT_2]_n$	$3d^0$			0	561(0)	487(0)
$[MnT_2]_n$	$3d^5$	5.89	8.5	0	587(0)	517(0)
$[CoT_2]_n$	$3d^7$	4.41	9.3	7.89	592(4)	530(7)
$[NiT_2]_n$	$3d^8$	2.94	8.9	11.32	611(22)	545(18)
$[CuT_2]$	$3d^9$	1.86	12.0	7.63 [b]	639(49)	589(59)
$[ZnT_2]_n$	$3d^{10}$			0	590(0)	533(0)
$[ScT_3]$	$3d^0$			0	583(0)	544(0)
$[TiT_3]$	$3d^1$		20.3	8.61	596(11)	541(−5)
$[VT_3]$	$3d^2$		18.6	15.56	621(34)	557(9)
$[CrT_3]$	$3d^3$	3.79	17.0	21.62	627(37)	565(15)
$[MnT_3]$	$3d^4$	4.74	21.0	13.36 [b]	602 [c](10)	566 [c](3)
$[FeT_3]$	$3d^5$	5.78	14.0	0	594(0)	555(0)
$[CoT_3]$	$3d^6$	diamag.	19.0	48.34 [d]	656(60)	585(25)
$[GaT_3]$	$3d^{10}$			0	607(0)	582(0)

[a] Values of ($\nu - \nu_0$) in parentheses. [b] Excluding Jahn–Teller stabilization. [c] Mean of doublet. [d] Excluding pairing energy.

tropolonates attain a maximum value at Cu(II) whereas the CFSE data would imply a maximum at Ni(II).

The electronic spectrum of [MnT_3] yields evidence [15] of tetragonal distortion. The unique feature of the infrared spectrum (Fig. 7) is the doubling of the two principal M–O bands. The band splitting is undoubtedly associated with the existence of two species of Mn–O bond length (and hence force constant) in the distorted molecule. Such band splitting in the spectra of nominally octahedral complexes of Mn(III) and Cu(II) has now been observed [16–18] for a sufficient number of ligand systems to be considered as diagnostic of tetragonal distortion.

Metal ions with $3d^4$–$3d^7$ configurations may occur in octahedral complexes with either spin-free or spin-paired configurations. The majority of ligands and ions favour the former configuration but Co(III) complexes are commonly spin-paired. The relationship between νM–L and $3d$-orbital population of the form established for metal tropolonates has now been shown to hold for a large variety of other ligands in complexes where the metal ions have the same spin states as exist in tropolonate complexes. Examples are metal acetylacetonates [17–19], metal β-ketoenolates [20–24], adducts of metal β-ketoenolates [25,26], salicylaldehyde complexes [27], salicylaldimine complexes [28–31], metal anthranilates [32], metal oxalates [33] and other systems [34]. In certain cases of these series of complexes, independent methods of assignment of νM–L have been applied and the level of qualitative agreement between these techniques and the crystal field approach is generally excellent. The consistency with which the relationship between νM–L and $3d$-orbital population is observed implies that the CFSE approach represents a powerful technique for the assignment of νM–L.

D. SPIN-PAIRING EFFECTS

The high crystal field strengths of the ligands 2,2'-bipyridine (bipy) and 1,10-phenanthroline (phen) have the effect of imposing spin-paired configuration on their Fe(II) complexes. In the series of complexes [$M(N–N)_3$](ClO_4)$_2$ (Fig. 9) where N–N represents either of the ligands bipy or phen, the normal CFSE order becomes deranged to Mn < Fe > Co < Ni > Cu > Zn. If the crystal field interpretation of metal–ligand frequencies is entirely valid, the variation in νM–L should reflect this modified sequence. The spectra (Fig. 10) exhibit [35] four significantly M-sensitive bands. Only the two bands near 400 cm^{-1} correspond with a region of ligand absorption. Assignment of the two M-sensitive bands below 400 cm^{-1} to νM–N is therefore indicated while the two bands above 400 cm^{-1} undoubtedly have νM–N character. The shift of the principal νM–N band exhibits a frequency variation with $3d$-orbital population (Fig. 11) which parallels the CFSE
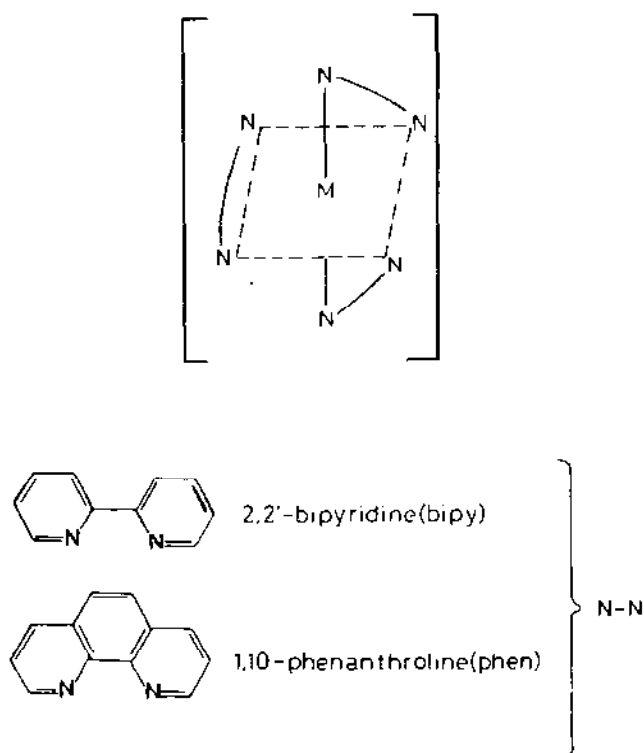
Fig. 9. Structure of metal complexes based on 2,2'-bipyridine and 1,10-phenanthroline ligands.

sequence calculated on the basis of spin-paired Fe(II). Both the stability constants (log β_3) and heats of ligations (ΔH) have been determined [36] for these complexes. Comparison of the dependence of these parameters with that of νM–N on $3d$-orbital population (Fig. 11) is strongly indicative of a common origin in determining their values.

Comparison of the spectra of the pairs of complexes [M(N–N)$_3$](ClO$_4$)$_2$ where M is Ni(II) and Cu(II) is highly informative with respect to the existence and extent of Jahn–Teller distortion in the Cu(II) complexes. The stability constants [36] of the bipy complexes are in the order Ni > Cu rather than the Irving–Williams [1] order Ni < Cu more generally observed in the presence of significantly distorted Cu(II) complexes. The calculated CFSEs of the Ni(II) and Cu(II) bipy complexes are 10.3 and 15.3 kK, respectively. Thus, if distortion occurs in the Cu(II) bipy complex, the associated stabilization would have to exceed 5 kK for the stability order Ni > Cu to be reversed. The only conclusion to be reached from the stability constant data is that the Cu(II) bipy complex is either not distorted or only weakly
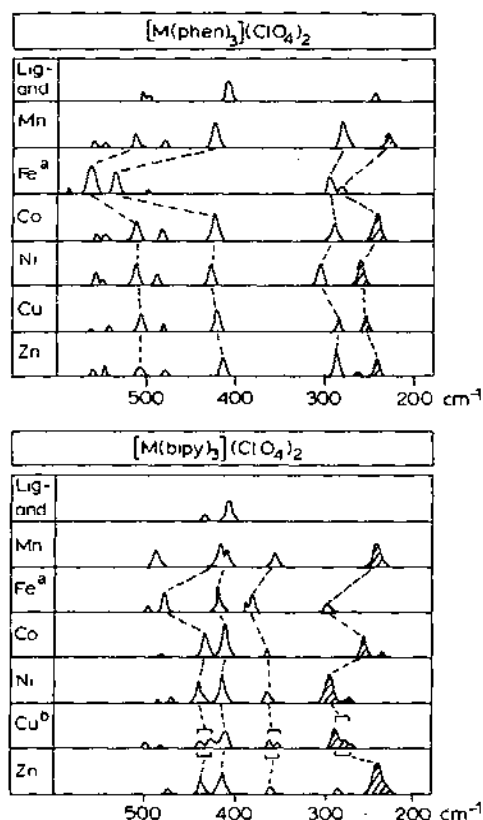
Fig. 10. Infrared spectra of $[M(N-N)_3](ClO_4)_2$ complexes. The principal $\nu M-N$ bands are shaded. [a] Spin-paired. [b] Jahn–Teller distorted.

distorted. From the infrared spectra, however, the distortion in the Cu(II) bipy complex is clearly observed (Fig. 10) since the principal $\nu M-N$ bands of the Ni(II) complex spectrum become doubled in the spectrum of the Cu(II) complex. The combined stability constant and infrared data therefore suggest that the $[Cu(bipy)_3](ClO_4)_2$ complex is tetragonally distorted but that the associated stabilization does not exceed 5 kK.

Extending this argument to the complexes $[M(phen)_3](ClO_4)_2$ (M = Ni, Cu) we note that their CFSEs are identical with those of the corresponding bipy complexes since

$$f(bipy)_3 = f(phen)_3 = 1.43 \tag{6}$$

There is no observable band splitting in the Cu(II) phen complex (Fig. 10) while $\log \beta_3$ is again in the order Ni > Cu. Thus, within the limits of detection by the infrared method, phen is unable to expand its bite (N–N

distance) sufficiently to accommodate the thermodynamically more favourable tetragonal structure. These differences are readily attributable to the presence of a fused-ring system in phen (Fig. 9) which confers greater steric rigidity than exists in bipy.

The effects of spin-pairing on $\nu M-L$ are also observable in a comparison [11] of the spectra of the tris(tropolonate) complexes of the first and second transition series metal(III) ions. The feature of interest here is the different spin states of the $3d^5$ Fe(III) and $4d^5$ Ru(III) complexes which are spin-free and spin-paired, respectively. From the data in Table 3, it is observed that the transformation: spin-free $[FeT_3]$ $(3d^5) \rightarrow$ spin-paired $[CoT_3]$ $(3d^6)$ is accompanied by a significantly greater increment in $\nu M-O$ and $(\nu-\nu_0)$ than spin-paired $[RuT_3]$ $(4d^5) \rightarrow$ spin-paired $[RhT_3]$ $(4d^6)$, as the relative increments in CFSE would require. Similar spin-pairing effects on $\nu M-L$ have been demonstrated [33] in the second transition series metal(III) acetylacetonates and the first transition series metal(III) cyanide complexes, $K_3[M(CN)_6]$.

The structural conclusions reached from studying the spectra of the metal(II) complexes of tropolone, bipy and phen may be used to determine
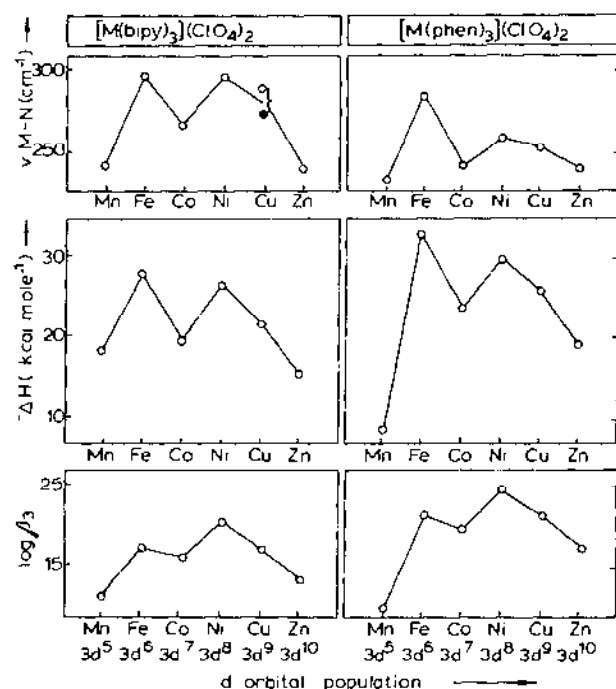

Fig. 11. Relationship between $\nu M-N$, ΔH, log β_3 and $3d$-orbital population for $[M(N-N)_3](ClO_4)_2$ complexes.

TABLE 3

Effects of spin-pairing on νM–O in tropolonate complexes

	[FeT$_3$]	[CoT$_3$]	[RuT$_3$]	[RhT$_3$]
Configuration	$3d^5$	$3d^6$	$4d^5$	$4d^6$
Spin state	spin-free	spin-paired	spin-paired	spin-paired
g(kK)	14	19	30	27
$-$CFSE[a] (kK)	0	29	52	56
νM–O (cm^{-1})	594	656	662	663
$(\nu-\nu_0)$(cm^{-1})	0	60	73	70
νM–O (cm^{-1})	555	585	573	580
$(\nu-\nu_0)$(cm^{-1})	0	25	47	48

[a] Including pairing energy.

the precise nature of the distortion in the mixed ligand complexes [CuT$_2$(N–N)]. The infrared spectra [11] of the complete series of complexes [MT$_2$(N–N)] (M = Mn, Co, Ni, Cu, Zn) in which the $3d^6$ and $3d^7$ complexes are spin-free, are depicted in Fig. 12. The strong band below 300 cm^{-1} is
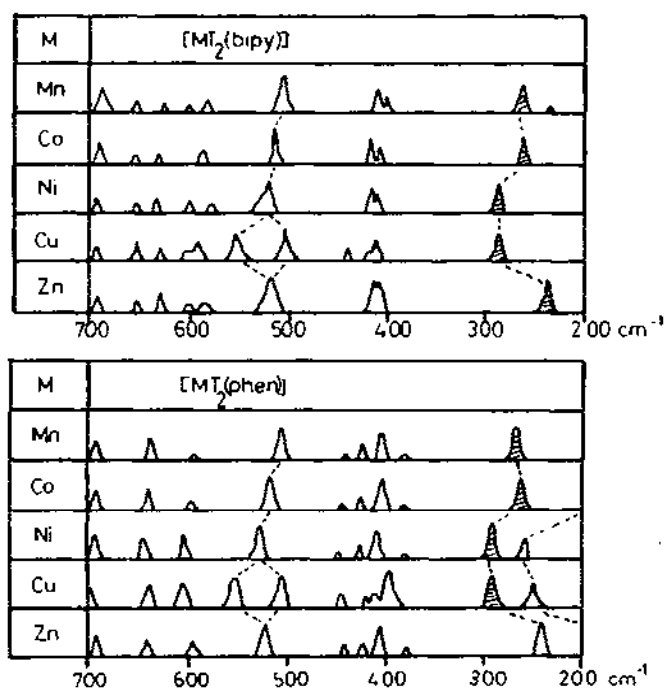

Fig. 12. Infrared spectra of [MT$_2$(N–N)] complexes. Linked, shaded bands are νM–N and linked, unshaded bands are νM–O.
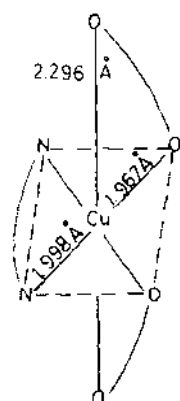
Fig. 13. Structure of the distorted [Cu(hfa)₂(bipy)] complex.

M-sensitive in the CFSE order Mn < Co < Ni > Zn. It corresponds in position with the principal νM–N band [35] of the complexes $[M(N-N)_3](ClO_4)_2$ and is therefore assigned to νM–N. The band within the range 560–500 cm^{-1}, which is also M-sensitive in the CFSE order Mn < Co < Ni > Zn, corresponds in position with one of the principal νM–O bands [6] in the complexes $[MT_2]_n$ and is therefore assigned to νM–O. Only the νM–O band is split in the spectra of the complexes $[CuT_2(N-N)]$, suggesting that the distortion involves elongation of the Cu–O bonds rather than the Cu–N bonds and therefore that the tropolonate anion is better able to expand its bite to accommodate tetragonal distortion than either bipy or phen. Support for this conclusion arises from the crystal structure [37] of the complex $[Cu(hfa)_2(bipy)]$ (hfa = hexafluoroacetylacetonate anion) which shows (Fig. 13) that distortion involves elongation of the axially-coordinated oxygen atoms of the hfa anion, the observed bond lengths being given in the formula. The spectrum [11] of this complex also shows splitting of νCu–O but not νCu–N.

E. METAL ANTHRANILATE SPECTRA

Anthranilic acid is a bidentate chelating ligand with both nitrogen and oxygen donor atoms. The metal(II) complexes of this ligand represent examples where the application of a combination of the isotopic labelling technique and the crystal field approach has been employed [32] to assign νM–N and νM–O (in using these labels, the probability of coupling between νM–N and νM–O and of coupling of each of these modes with ligand vibrations is acknowledged). The metal(II) anthranilates have a nominally octahedral structure consisting of a *trans*-planar arrangement of two anth-
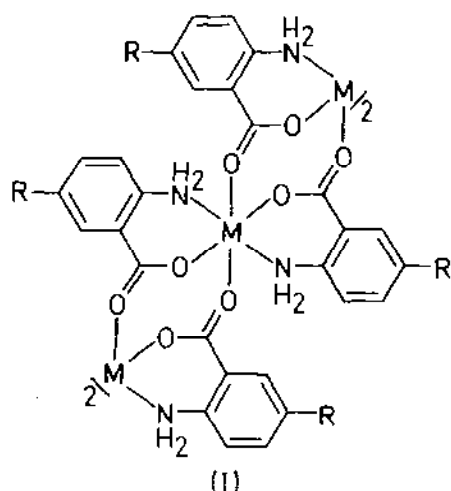
Fig. 14. Structure of the metal anthranilates.

ranilate ligands about the metal ion with the *trans*-axial positions occupied by those oxygen atoms of neighbouring molecules which are not involved in chelation. Figure 14 illustrates the partial structure (R = H).

The spectra of sodium anthranilate and the complexes of the metal(II) ions Mn, Co, Ni, Cu and Zn are shown in Fig. 15. The procedure in assigning νM–N is to seek a band which satisfies three criteria: significant ^{15}N-sensitivity (on labelling of the amino group with the ^{15}N-isotope); significant M-sensitivity (on varying the metal ion, the order of M-depen-
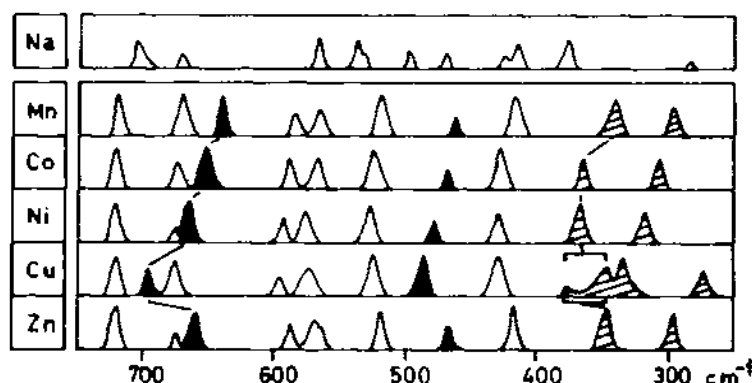

Fig. 15. Infrared spectra of metal anthranilates. Solid, linked bands are principal νM–N; solid, unlinked bands are coupled νM–N. Shaded, linked bands are principal νM–O; shaded, unlinked bands are coupled νM–O.

dence following the CFSE sequence Mn < Co < Ni > Zn); and occurrence of the band within a region free from ligand absorption. The last of these criteria would strengthen the assignment but is not necessary to it since there may be fortuitous coincidence of ligand and νM–N bands. One component of the band pair within the range 700–600 cm^{-1} (the solid, linked component in Fig. 15) is the only band which satisfies each of these criteria. It is therefore assigned as the principal νM–N band. The other component is neither ^{15}N- nor M-sensitive and its position corresponds with a ligand band observed in the spectrum of the sodium salt.

A band within the range 500–450 cm^{-1} (the solid, unlinked band in Fig. 15) may also be assigned to νM–N on the grounds of its ^{15}N- and M-sensitivity, the latter being in the CFSE order. This band differs from the principal νM–N band by its occurrence in a region of ligand absorption and by its smaller M-sensitivity. Since the ligand band within this range (assigned to δCCC + δCCN) is not repeated in the spectra of the complexes, it is concluded that this band represents νM–N coupled with the ligand vibration.

To assign νM–O, use is made of the effects of Jahn–Teller distortion on the spectrum of the Cu(II) complex. The crystal structure [38] of cadmium glycinate (which is analogous with that of an anthranilate complex) exhibits axially coordinated oxygen atoms only 0.2 Å farther from the Cd(II) ion than those in the planar chelate rings. No significant splitting of νM–O would be expected in the presence of such minor distortion. However, in Cu(II) anthranilate we expect such distortion to be much more extensive in which case the Cu(II) ion will be bound to oxygen by two species of Cu–O bond but only one species of Cu–N bond. The bonding situation is analogous with that of the complexes [CuT$_2$(N–N)] discussed in the previous section and splitting of νCu–O bands but not νCu–N is expected. In Fig. 15 it is observed that the pair of adjacent (shaded) bands within the range 400–200 cm^{-1} becomes a set of four bands in the spectrum of the Cu(II) complex, suggesting their assignment to νM–O. Both bands are highly M-sensitive in the CFSE sequence. The higher frequency component of the band pair occurs in a region free from ligand absorption and has a very small ^{15}N-sensitivity. It is therefore assigned as the principal νM–O band. The lower frequency component is significantly ^{15}N-sensitive and is undoubtedly coupled with the weak ^{15}N-sensitive ligand band near 300 cm^{-1} (assigned to δCCN).

The assignments of νM–N and νM–O receive support [32] from observations of the effects of substitution at the 5-position (R in Fig. 14) of the anthranilate aryl ring on the spectra (Fig. 16). The shifts in the metal–ligand vibrations imposed by the substituents have been rationalized in terms of the predicted influence of the electronic effects of these substituents on the force
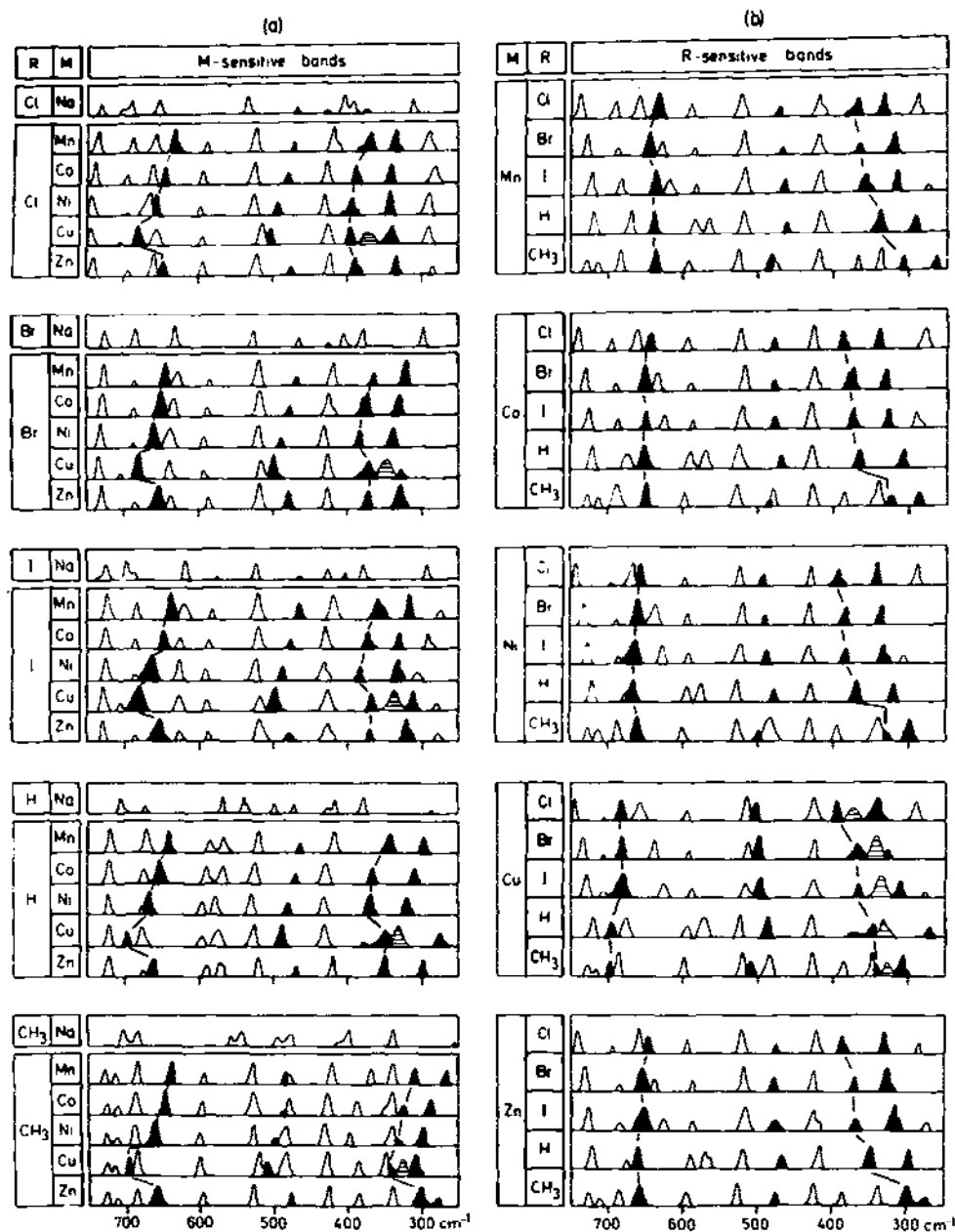
Fig. 16. Infrared spectra (250–750 cm⁻¹) of metal anthranilate complexes showing effects of (a) metal ion substitution, and (b) ligand substitution. Solid peaks (linked): principal νM–N and νM–O bands; solid peaks (unlinked): coupled νM–N and νM–O bands; shaded peaks: additional νM–O bands in Cu(II) complexes.
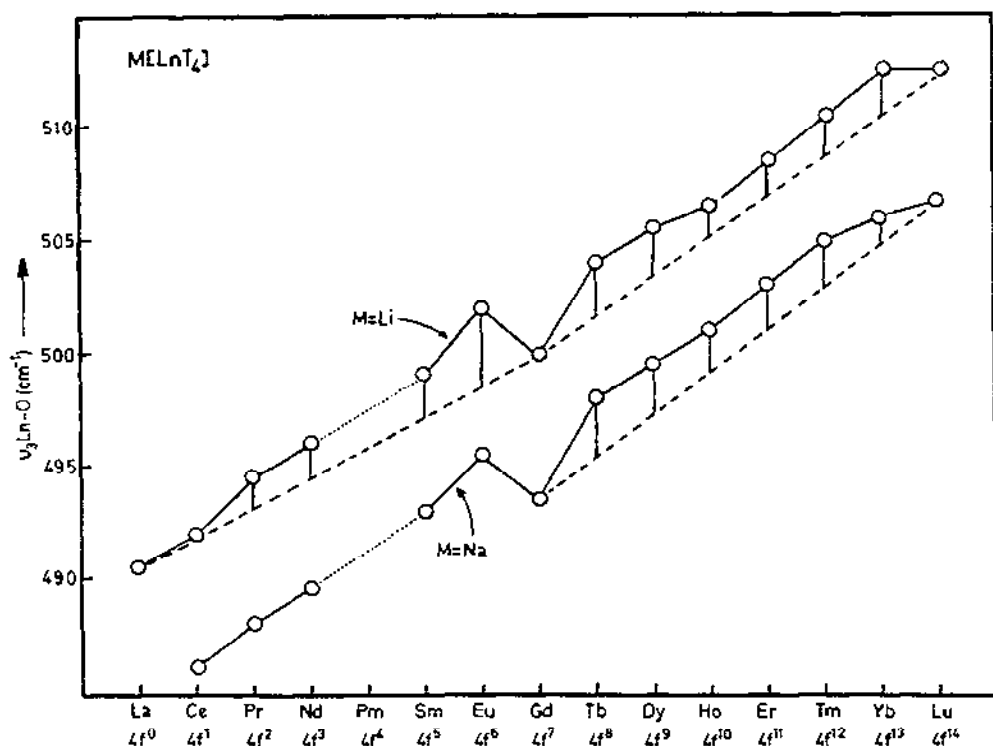
Fig. 17. Relationship between νLn–O and $4f$-orbital population for M[LnT$_4$] complexes (M = Li, Na). The dashed lines represent (ν_0) and the vertical lines represent ($\nu - \nu_0$).

constants of the M–O and M–N bonds. A combination of the isotopic labelling and crystal field techniques has been applied [28–30] to the assignment of νM–N and νM–O in complexes of N-alkyl- and N-aryl-salicylaldimines with similarly encouraging results to those realized for the metal anthranilates (see Section I).

F. LANTHANIDE TROPOLONATE SPECTRA

Crystal field effects are much smaller in complexes of the lanthanide ions than in complexes of the ions of the main transition series. In complexes of $4f^n$ ions, cation size becomes the predominant feature determining complex stability. Although complexing ligands are known to have only very small effects on the positions of the electronic absorption bands in lanthanide complexes, the proposal [39] that crystal field splitting of the $4f$ orbitals may be sufficient to influence the enthalpies of complex formation has been

substantiated, for instance, by the thermodynamic data of Campbell and Moeller [40,41] on the lanthanide tropolonate complexes.

Yatsimirskii and Kostromina [42] have shown that the variation of CFSE with 4f-orbital population has the double-humped shape characteristic of 3f^n complexes with minima at the 4f^0, 4f^7 and 4f^{14} configurations, which are not stabilized by the crystal field. Experimental support for theoretical predictions of crystal field stabilization in lanthanide complexes can presently be sought only in the broadest qualitative sense since no means exists at present for measurement of the magnitude of the crystal field splitting. Such support has recently been obtained [7,8] from the infrared spectra of the lithium salts of the 8-coordinate tetrakis(tropolonato) lanthanide(III) complexes, Li[LnT$_4$] (Ln = lanthanide ion). Identical band patterns are
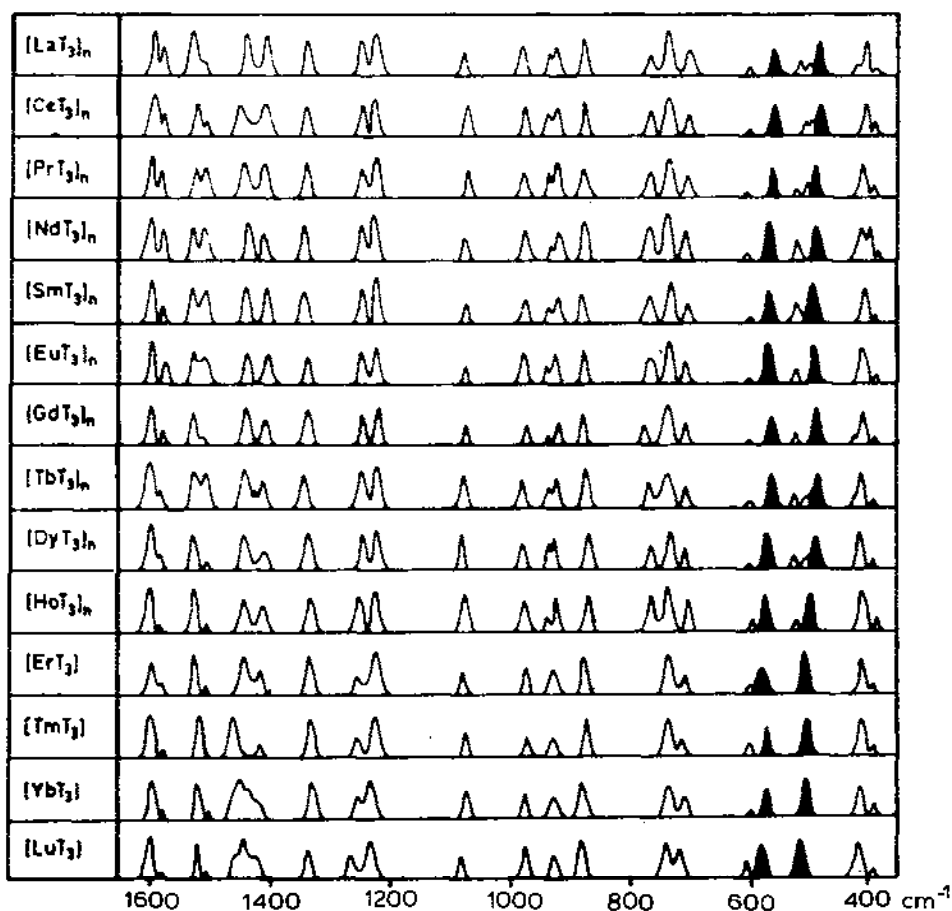

Fig. 18. Infrared spectra of [LnT$_3$]$_n$ complexes. The principal νLn—O bands are solid.

exhibited by the infrared spectra of the fourteen complexes, showing that they are isostructural. Maximum sensitivity to the Ln(III) ion is exhibited by the band within the range 520–490 cm^{-1} which is accordingly assigned as the principal νLn–O band. The variation of νLn–O with $4f$-orbital population (Fig. 17) yields the double-humped curve expected to arise from the crystal field effects with minima at the $4f^0$, $4f^7$ and $4f^{14}$ configurations. The sodium salts, Na[LnT$_4$], exhibit a similar trend but the La(III) complex could not be synthesized. The mean value of $(\nu-\nu_0)$ which represents the crystal field contribution to νLn–O, is approximately one-twentieth of the mean value of $(\nu-\nu_0)$ in the complexes [MT$_3$] where M is a metal(III) ion of the first transition series. This ratio is in good accord with the results of an analysis [43] of the thermodynamic parameters of the diglycollate and dipicolinate complexes of the $4f^n$ ions which reveals that crystal field effects operate for the lanthanide ions on a scale between one and two factors of ten smaller than for $3d^n$ ions.

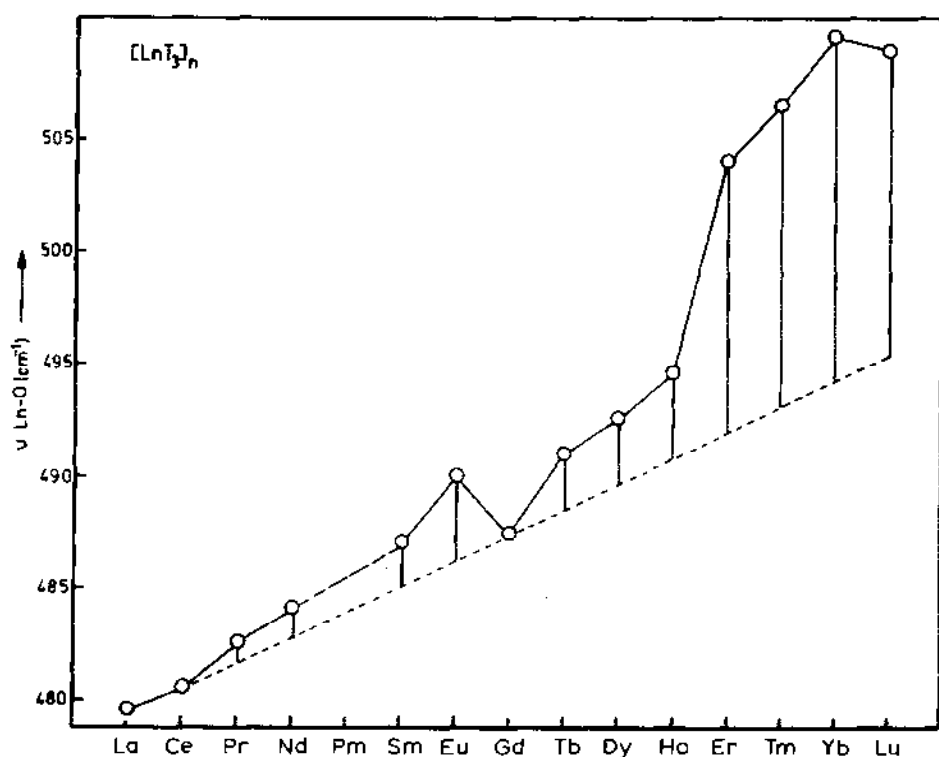The infrared spectra of the lanthanide(III) tris(tropolonate) complexes of

Fig. 19. Relationship between νLn–O (within the range 510–470 cm^{-1}) and $4f$-orbital population for the complexes [LnT$_3$]$_n$.

empirical formula [LnT₃] (Fig. 18) are of interest in relation to their proposed [44] structures which suggest that the complexes of the ions La(III) $(4f^0)$ through Ho(III) $(4f^{10})$ have a polymeric lattice with coordination number exceeding six (probably eight) while the last four ions, Er(III) $(4f^{11})$ through Lu(III) $(4f^{14})$ yield monomeric 6-coordinate complexes. The decrease in coordination number preceding Er(III) should lead to a marked increase in νLn–O since the bonding capacity of the lanthanide ion is distributed over fewer Ln–O bonds in the last four complexes. The bands within the range 600–450 cm^{-1} exhibit such an increase (Fig. 19) and are also the bands exhibiting maximum sensitivity to the coordinated Ln(III) ion. Both observations suggest that they are the principal Ln–O bands while the change in coordination preceding Er(III) is also reflected by a change in band patterns (Fig. 18).
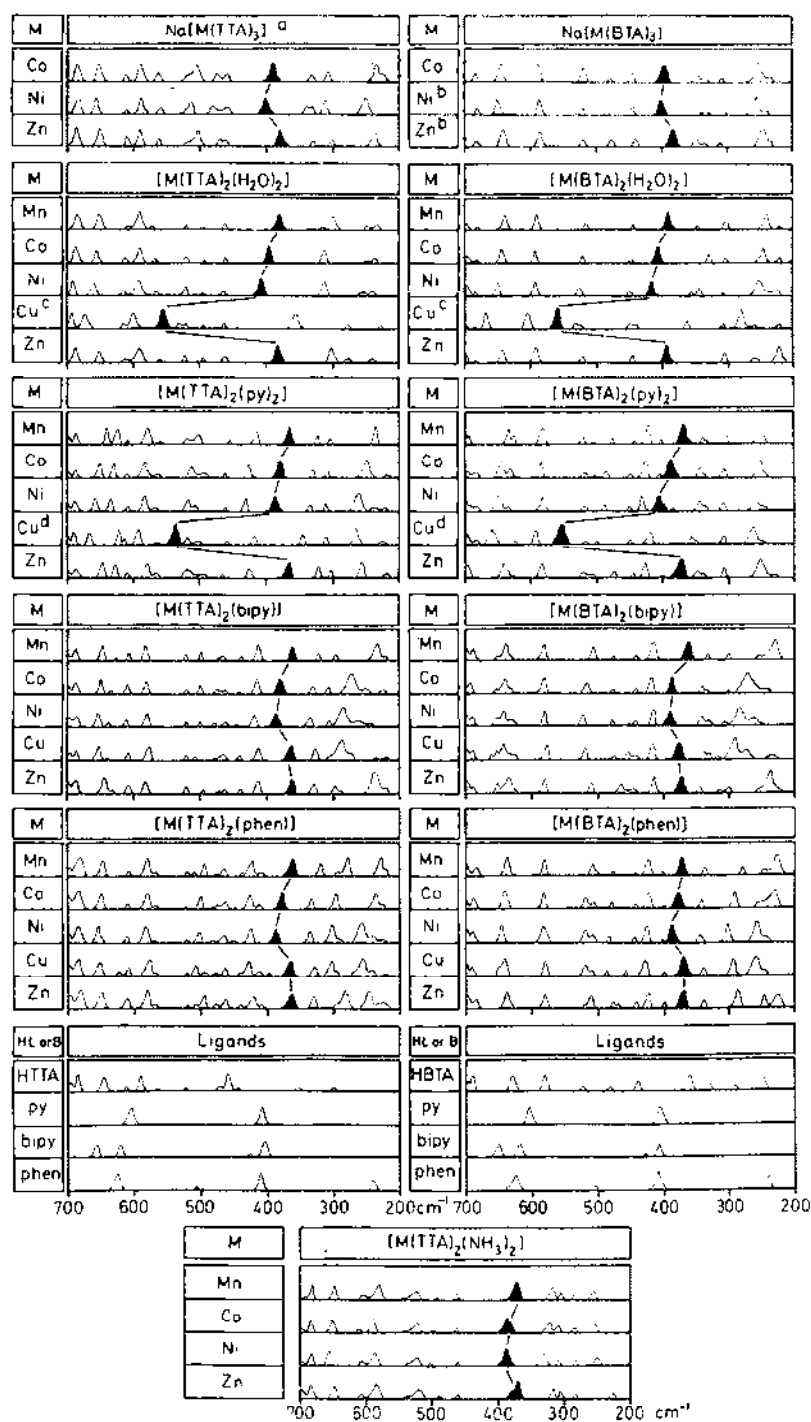
G. A SPECTROCHEMICAL SERIES OF LIGANDS FROM INFRARED SPECTRA

The infrared spectra of a large range of compounds of general formula Na[ML₃] or [ML₂B] has been determined with a view to arranging the ligands B in a spectrochemical series [45]. In these series, M is a divalent ion of the first transition series, L is the α-thenoyltrifluoroacetonate (TTA) or benzoyltrifluoroacetonate (BTA) anion and B is 2 H₂O, 2 NH₃, 2-pyridine, 2,2'-bipyridine or 1,10-phenanthroline. Within each series of complexes with common L or B, the infrared band near 400 cm^{-1} which exhibits maximum sensitivity to the coordinated metal ion and which generally occurs in a region free from ligand absorption is assigned to νM–O. The sensitivity to the coordinated metal ion is in the sequence of CFSE values (Fig. 20).

If the complex anion of the compounds Na[ML₃] is represented as [ML₂B]$^-$ (in this case B≡L) then the various series of complexes studied may be represented by the single general formula [ML₂B]$^{n-}$. In the complexes of Mn(II), compounds of this formula were synthesized with B = 2 H₂O, 2 NH₃, (NH₃ + H₂O), 2 py, TTA, BTA, bipy and phen. Figure 21 shows that νM–O in this series of complexes moves in the sequence 2 H₂O > (NH₃ + H₂O) > TTA > 2 NH₃ > 2 py > bipy ≈ phen. The calculated f-values (from $10Dq = fg$) of these ligand combinations are in the same sequence, thus establishing the usefulness of infrared spectra to the problem of crystal field strength determination in these complexes.

H. SALICYLALDEHYDE COMPLEXES

The structure of the anhydrous salicylaldehyde complexes of Co(II), Ni(II) and Cu(II) have been extensively investigated. Although originally
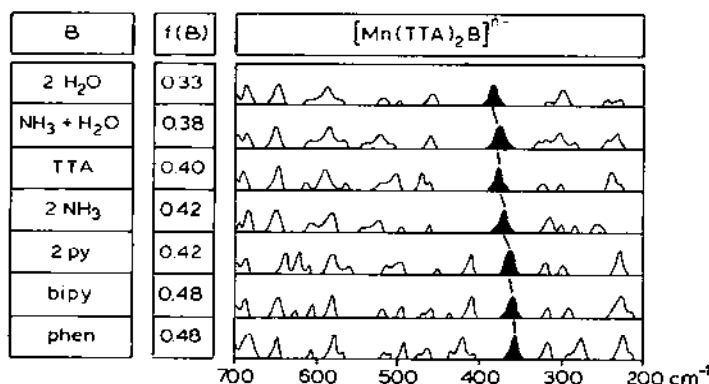
B	f(B)	$[Mn(TTA)_2B]^{n-}$		
2 H$_2$O	0.33			
NH$_3$ + H$_2$O	0.38			
TTA	0.40			
2 NH$_3$	0.42			
2 py	0.42			
bipy	0.48			
phen	0.48			

Fig. 21. Infrared spectra (700–200 cm^{-1}) of manganese(II) complexes $[Mn(TTA)_2B]^{n-}$. Solid bands are ν(Mn–O).

considered to be tetrahedral or planar [46–48], evidence from X-ray diffraction studies [49,50], electronic spectra and magnetic moments [50–52] firmly establishes polynuclear octahedral structure for the Co(II) and Ni(II) derivatives and very nearly square planar coordination [50,53,54] in the Cu(II) chelate. The structures of these complexes are therefore entirely analogous with the acetylacetonates and tropolonates of these ions. There is generally a band-for-band correspondence in the IR spectra of the Co(II) and Ni(II) complexes of the six variously-substituted salicylaldehydes discussed here (Fig. 22), supporting their isostructural character, while the Cu(II) complexes yield unique band patterns in accordance with their planar structure.

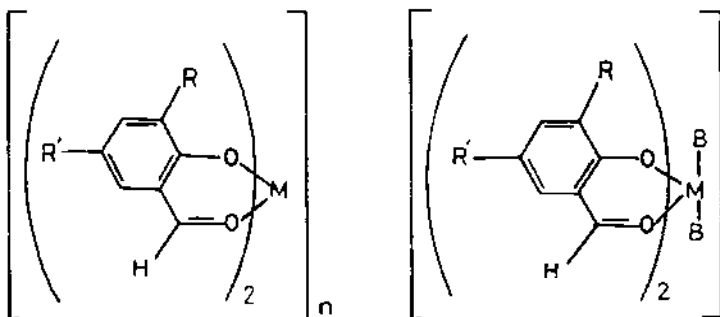In a series of complexes of an identical ligand with octahedral Co(II) and

Fig. 22. Structures of salicylaldehyde complexes (left) and dibase adducts (right).

Fig. 20. Infrared spectra (700–200 cm^{-1}) of complexes Na[ML$_3$] and [ML$_2$B]. Solid bands are ν(M–O). [a] The spectrum of Na[Mn(TTA)$_3$] is given in Fig. 21; [b] monohydrate; [c] anhydrous [CuL$_2$]; [d] monopyridine complex [CuL$_2$(py)].

Ni(II) and square planar Cu(II), the CFSE order is identical with the Irving–Williams stability order, viz. Co < Ni < Cu. The spectra of the anhydrous salicylaldehyde complexes (Fig. 23) exhibit more than one band below 650 cm^{-1} with metal-sensitivity in this order and which may therefore be assigned to variously coupled M–O stretching vibrations. The doublet within the range 520–620 cm^{-1} exhibits the maximum sensitivity to the metal ion in the order Co < Ni < Cu and generally occurs in a region free from ligand vibrations. These two bands are therefore assigned as the principal νM–O bands.

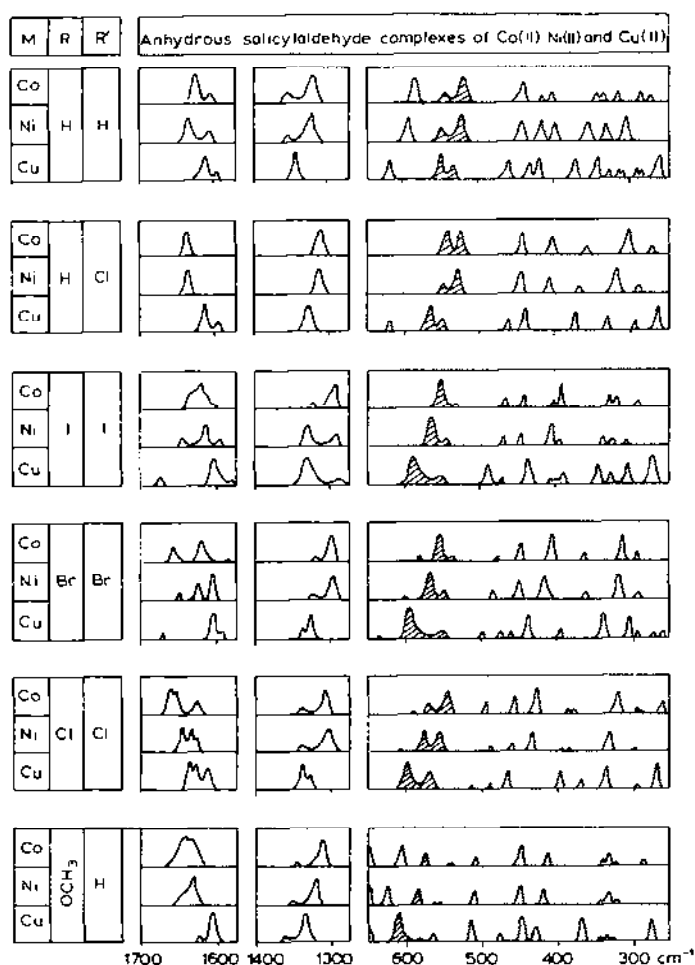The values of νM–O are some 50 cm^{-1} lower than those of the principal

Fig. 23. Effect of metal ion substitution on the infrared spectra of anhydrous salicylaldehyde complexes (Fig. 22). Shaded bands: νM–O.

νM–O bands in the structurally analogous acetylacetonates. This difference is consistent with the relative stability constants [55] which are about 25% lower for the salicylaldehyde complexes of Co(II) and Ni(II) than the values for the analogous acetylacetonates. Thus salicylaldehyde would seem to occupy a position in the spectrochemical series close to water which has a ligand field strength approximately 20% lower than that of acetylacetone. [56].

Introduction of substituents into the aryl ring of the salicylaldehyde complexes (Fig. 24) is expected to shift νM–O if the electronic effects of the substituents are transmitted to the chelate ring. In the anhydrous complexes and in the bis(aquo) and bis(pyridine) adducts, substantial shifts in the bands assigned to νM–O on the basis of metal ion substitution occur in the substituent sequence: H < 5-Cl < 3,5-di-1 < 3,5-di-Br < 3,5-di-Cl < 3-OCH$_3$. Except for the 5-Cl substituent (for which νM–O is slightly lower than expected) this sequence is also the order of electron releasing resonance capacities of the substituents. A quantitative index of this effect is provided by Taft's [57] resonance polar parameter, $\sigma_p - \sigma'$. The consistency with which this substituent sequence is followed by νM–O in the seven sets of complexes containing the 6 substituted salicylaldehydes represented in this study is considered to provide strong support for the νM–O assignments proposed.

The dependence of νM–O on a resonance rather than an inductive parameter suggests that the mesomeric effects of the substituents predominate in determining the M–O bond order. Since the transmission of these effects through both chelate rings is dependent on interligand conjugation, it is likely that metal–ligand π-bonding plays an important role in stabilizing these complexes.

The Co(II) and Ni(II) complexes of the six salicylaldehydes each formed stable dibase adducts with water and pyridine. X-ray diffraction studies [58,59] have shown that Ni(II) salicylaldehyde dihydrate is *trans*-octahedral and isomorphous with the Co(II) analogue. The band patterns below 650 cm^{-1} of the pairs of Co and Ni complexes with common B and R, are sufficiently similar to suggest that *trans*-octahedral coordination occurs in all the Co(II) and Ni(II) adducts. Furthermore, the values of νM–O are, without exception, in the order Co < Ni, as expected from their relative CFSE's assuming octahedral coordination.

The fact that no dramatic shift in νM–O accompanies the transformation of the anhydrous complexes into their dihydrates implies that no change in coordination number accompanies the transformation. In the absence of any change in ligand composition, increased coordination number causes a considerable low-frequency shift of νM–L. This is exemplified, for instance [60], by the transformation of mononuclear tetrahedral [Co(py)$_2$Cl$_2$] (νCo–N = 252 cm^{-1}) into polynuclear octahedral [Co(py)$_2$Cl$_2$]$_n$ (νCo–N =
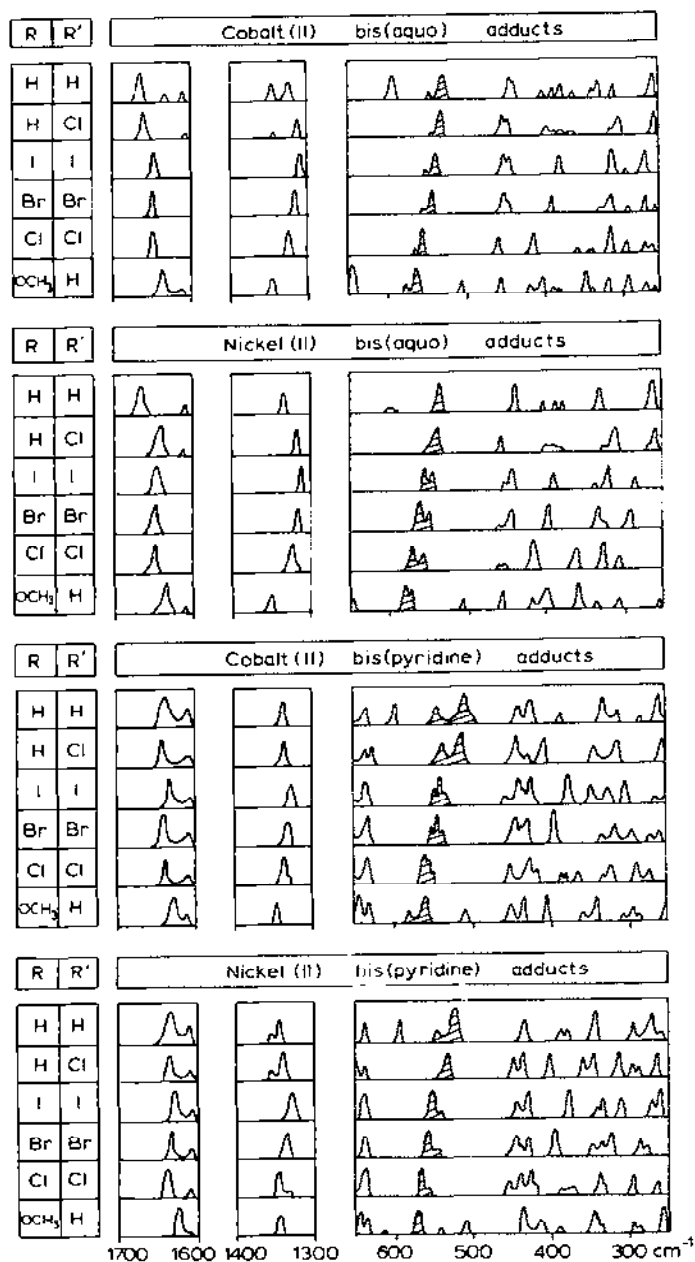
Fig. 24. Effect of ligand substitution on the infrared spectra of bis(aquo) and bis(pyridine) adducts of Co(II) and Ni(II) salicylaldehyde complexes. Shaded bands: νM–O.

224 cm^{-1}). The transformation $[M(sal)_2]_n \rightarrow [M(sal)_2(H_2O)_2]$ does involve a change in ligand composition but the ligand field strength of the ligand introduced (water) is comparable with that replaced (salicylaldehyde) so that no significant shift in $\nu M-O$ is expected to accompany this transformation if the anhydrous complex is 6-coordinate. Therefore, the generally small shifts observed (mean shift $+2$ cm^{-1}) in $\nu M-O$ on hydration are consistent with polynuclear octahedral coordination in the anhydrous complexes.

Pyridine has a ligand field strength some 25% greater than that of water. It is known [45,61] that an inverse relationship exists between the ligand field strength of the adducted base and $\nu M-O$ in the adducts of metal acetylacetonates and tropolonates (i.e., strengthening of the metal–adduct bond occurs at the expense of the metal–chelate bonding). Assuming this to hold for the salicylaldehyde complexes also, a decrease in $\nu M-O$ is expected to accompany the transformation $[M(sal)_2(H_2O)_2] \rightarrow [M(sal)_2(py)_2]$. Twelve such transformations are exemplified in the present study. In every case, a decrease in $\nu M-O$ (mean shift -9 cm^{-1}) is observed.

In the course of this study we isolated one example of a mixed-adduct species comprising one pyridine and one water molecule: $[Co(5-Cl-sal)_2(H_2O)(py)]$. Consistent with the foregoing discussion, the $\nu M-O$ values for this complex (540, 519 cm^{-1}) are intermediate between those for the bis(aquo) (550, 530 cm^{-1}) and bis(pyridine) (535, 512 cm^{-1}) adducts.

Salicylaldehyde complexes differ from acetylacetonates (but resemble tropolonates) in having two different C–O bond lengths in the chelate ring. This feature is undoubtedly associated with the relative degree of bond fixation implied by the benzenoid form which is likely to provide a greater contribution to the resonance hybrid than the non-benzenoid form (Fig. 25). We therefore expect to find IR bands distinctive of the aldehyde carbonyl ($\nu C=O$) and the phenolic carbonyl ($\nu C-O$) groups.

The band of highest intensity between 1600 and 1700 cm^{-1} has been empirically assigned to $\nu C=O$. Except for the complexes with two halogen substituents, metal ion and ligand substitution cause the frequency of this band to decrease as $\nu M-O$ increases. In the complexes with two halogen substituents, $\nu C=O$ and $\nu M-O$ shift in parallel in the halogen sequence I < Br < Cl. This feature is probably associated with the fact that the

Fig. 25. Benzenoid (left) and non-benzenoid (right) forms of salicylaldehyde complexes.

halogens are π-electron donors and σ-electron acceptors.

The effect of the replacement of water by pyridine in the adducts is always to decrease νC=O and generally to increase νC–O. The depletion of the electron density of both the M–O and C=O bonds by pyridine adduction is consistent with the π-acceptor properties of pyridine. Similar effects have been observed [62] for the pyridine adducts of uranyl β-ketoenolates.

Within the range 1300–1350 cm^{-1}, a strong band (or doublet) appears which is assigned to the phenolic νC–O, principally on the basis that its dependence on metal ion substitution, ligand substitution and pyridine adduction is generally the inverse of νC=O. The frequency of this band is, furthermore, practically identical with that of the similarly assigned band in Co(II) and Ni(II) tropolonates in which it occurs at 1340 cm^{-1}.

The spectra of the pyridine adducts are complicated by the presence of pyridine vibrations. At least two bands below 700 cm^{-1} are unique to the spectra of the pyridine adducts. These occur near 630 and 430 cm^{-1} and are practically insensitive to metal ion or ligand substitution. They are firmly assigned to pyridine vibrations, being observed [61] at almost identical positions in the spectra of pyridine adducts of metal acetylacetonates and tropolonates. No bands in the spectra of the pyridine adducts can be attributed to νM–N. Even the relatively firmly bound pyridine in the complexes [M(py)$_2$Cl$_2$]$_n$ has νM–N below 250 cm^{-1} [62]. In the adducts, these bands are, therefore, likely to occur beyond our range of measurement.

I. SALICYLALDIMINE COMPLEXES

Assignments of νM–N for the complexes of N-aryl salicylaldimines (Fig. 26; M = Co, Ni, Cu, Zn) have been made by ^{15}N-labelling of the imine nitrogen atom while νM–O has been assigned empirically. In seeking substantiation for the assignment of νCu–N proposed on the basis of ^{15}N-labelling, use has been made of the established relationship between CFSE and νM–L for transition metal complexes. Knowledge of the basic structures of the complexes is a prerequisite to this method of assignment. All currently
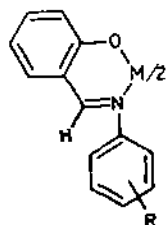
Fig. 26. Structure of N-aryl salicylaldimine complexes.

available structural evidence [63] points to tetrahedral coordination in the Co(II) and Zn(II) chelates of *N*-aryl Schiff bases while the Cu(II) complexes have nominally square planar coordination although minor deviations from true planarity commonly occur. Crystal field theory predicts that a series of three complexes with identical ligand composition containing tetrahedral Co(II) and Zn(II) and square planar Cu(II) will have CFSEs in the order Co < Cu > Zn. Accordingly, any band assigned as νCu–N is expected to exhibit a similar order of frequency variation on substitution of Co(II) or Zn(II) for Cu(II). With only one exception, the frequencies of the bands assigned to νCu–N reflect the predicted CFSE sequence for six differently substituted salicylaldimine complexes (Fig. 27).

A further test of the assignments is possible by extending this method to include Ni(II) Schiff base complexes of known structure. Crystallographic studies [63] have confirmed that *N*-phenylsalicylaldimine yields square planar complexes with Ni(II) and Cu(II). Crystal field theory predicts the stability order Ni > Cu for this pair of complexes since the orbital of highest energy is necessarily occupied in the Cu(II) chelate but is unoccupied in the diamagnetic Ni(II) analogue. The νCu–N bands are observed to exhibit this frequency order (Fig. 27). It is now useful to examine the spectra of a pair of complexes (M = Ni, Cu) for which the opposite stability order, i.e., the Irving–Williams stability sequence, Ni < Cu, is expected. The chelates of *N-p*-tolylsalicylaldimine ($R = p$-CH$_3$) are appropriate since the paramagnetic Ni(II) compound has [63] trinuclear octahedral structure while the Cu(II)
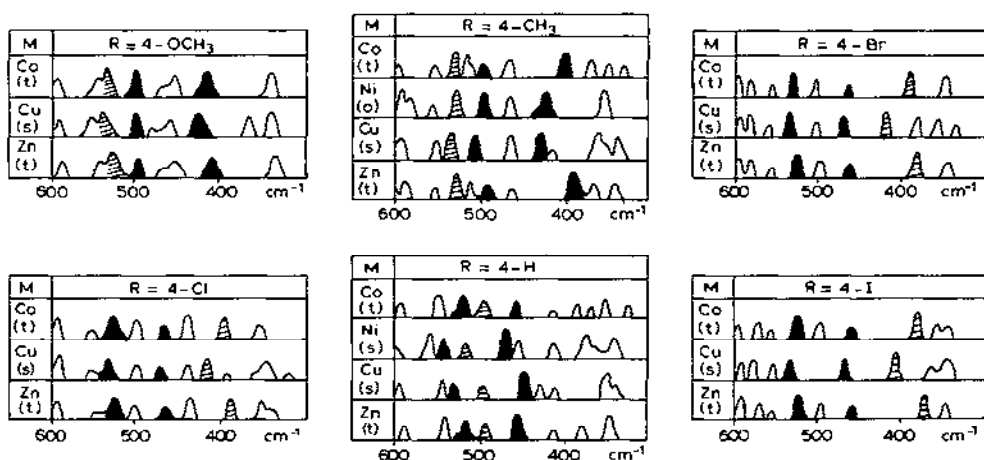

Fig. 27. Effect of metal ion substitution on infrared spectra of metal(II) salicylaldimine complexes (Fig. 26). Solid peaks: νM–N; shaded peaks: νM–O (tentative). Structures: *t* = tetrahedral; *s* = square planar; *o* = octahedral.

analogue is square planar. The change in the stability sequence is reflected by the frequency shifts observed for both bands assigned to $\nu M-N$ (Fig. 27).

Next, we examine the effect of varying the N-aryl substituent (R) in the Cu(II) complexes on the IR spectra. The two bands assigned to $\nu Cu-N$ on the basis of the isotopic labelling and metal-ion substitution studies both shift to higher frequency with increased electron withdrawing capacity of the substituents (Fig. 28). Since electron withdrawing substituents would facilitate $Cu \rightarrow N$ π-bonding, this result is not surprising. As concluded for the free bases, it is unlikely that the electronic effect is transmitted via the conjugation of the chelate ring, since $\nu C=N$ and $\nu C-O$ are insensitive to substitution in the N-aryl ring. In this connection it is interesting to observe

M	σ^-	M = Cu
4 -OC$_6$H$_5$	-0.32	
4 -OCH$_3$	-0.27	
4 -OC$_2$H$_5$	-0.25	
4 - CH$_3$	-0.17	
4 -C$_2$H$_5$	-0.15	
4 -C$_6$H$_5$	-0.01	
H	0	
4 -F	+0.06	
4 -Cl	+0.23	
4 -Br	+0.23	
4 -I	+0.28	
4 -CO$_2$C$_2$H$_5$	+0.45	
4 -COCH$_3$	+0.52	
4 -CN	+0.63	

600 500 400 300 cm^{-1}

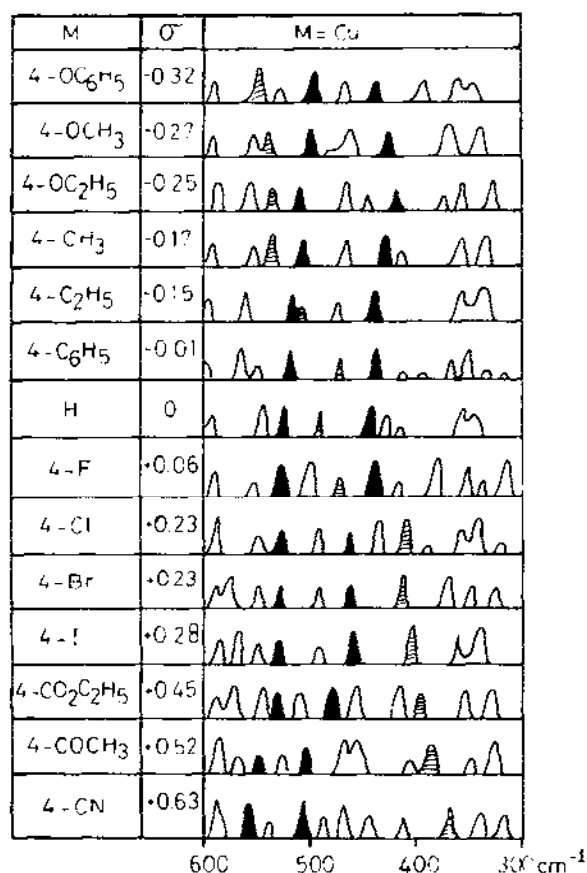Fig. 28. IR spectra of 4-substituted N-aryl salicylaldimine complexes of Cu(II) (Fig. 26; M = Cu). Solid peaks: $\nu Cu-N$; shaded peaks: $\nu Cu-O$.

that (by contrast with *para*-substitution) *meta-N*-aryl substituents induce very little shift in νCu–N. Since the electronic effects of *meta* substituents are transmitted almost entirely by an inductive mechanism, this suggests that the transmission of the substituent effects in the Schiff base complexes is propagated largely by a mesomeric mechanism. This conclusion was further examined in two ways. Firstly, it is found that two similar *meta* substituents, as in the 3,5-dibromo-substituted complex, yield values of νCu–N which are closely similar to those observed for the *meta*-bromo complex. Secondly, where a *meta* substituent is present in addition to a *para*-methyl substituent, as in the 3,4-di-CH$_3$-, 3-Cl, 4-CH$_3$- and 3-NO$_2$, 4-CH$_3$-substituted complexes, the values of νCu–N are similar to those of the *para*-methyl-substituted complex.

Corresponding studies have been made on *N*-aryl salicylaldimines substituted in both aryl rings [64]. The complexes have the general formula indicated in Fig. 29. The structures of these complexes are likely to be tetrahedral for M = Co, Zn and square planar for M = Cu. Crystal field theory predicts a stability order Co < Cu > Zn for these structures. Figure 30 illustrates the infrared spectra for a series of complexes with R = R' = Br (or R = OCH$_3$, R' = H) and varying X for each metal ion: Co, Cu, Zn. It is observed that the band near 450 cm^{-1} which exhibits maximum sensitivity to ^{15}N-labelling is also the most M-sensitive band in the spectra and occurs in the M sequence Co < Cu > Zn. So far as the substituent dependence of νM–N is concerned the strong π-electron releasing capacities of the substituents R and R' (measured by Taft's [65] resonance polar parameter, $\sigma_p - \sigma'$) cause νM–N to shift to higher frequency.

The transmission of the electronic effects of the R and R' substituents to the chelate ring may be facilitated or suppressed by the X-substituents in the *N*-aryl ring according to the electron withdrawing or releasing capabilities of X. The mechanism of transmission of the electronic effects of X through the
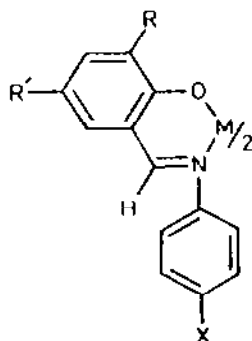

Fig. 29. Structure of salicylaldimine complexes substituted in both aryl rings.
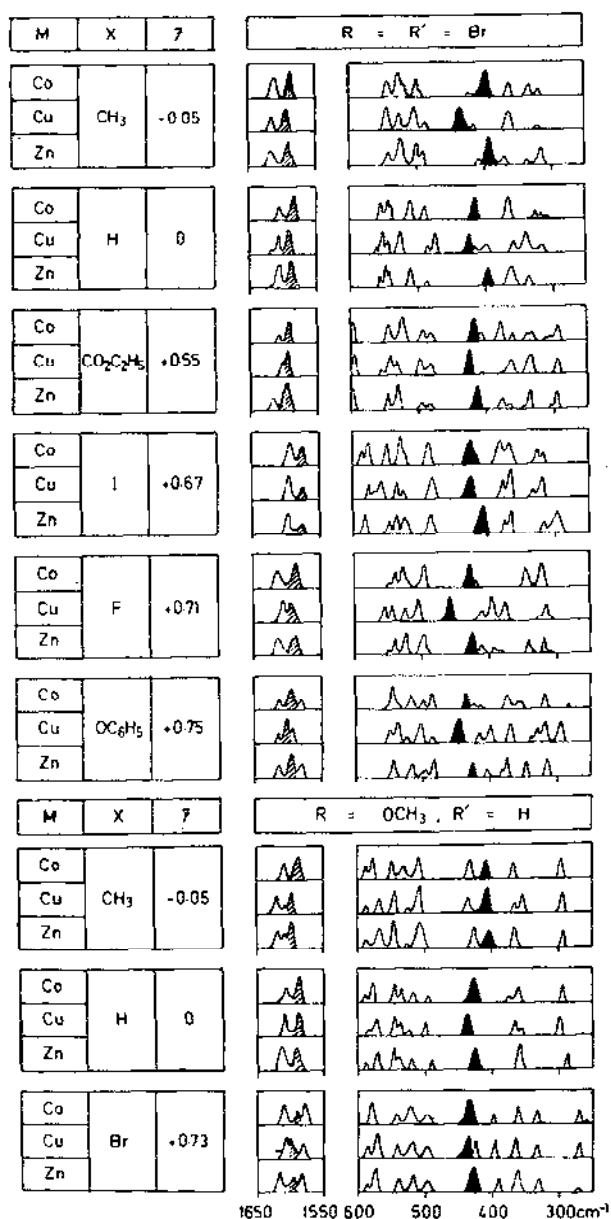
Fig. 30. Infrared spectra (1650–1550 and 600–250 cm^{-1}) of 3,5-dibromo- and 3-methoxysalicylaldimine complexes showing M- and X-sensitive bands. Shaded peaks: principal νC=N bands; solid peaks: νM–N.

molecule may be mesomeric or inductive or may occur by a combination of both processes. Recently, Swain and Lupton [66] have achieved a quantitative separation of the field (largely inductive) and resonance (largely mesomeric) capacities of organic substituents. The values of νM–N for the series of salicylaldimine complexes with common M, R and R' are found to be related to Swain and Lupton's field parameter (F) and not in any obvious way to the resonance capacities of the substituents. Inductively electron withdrawing X-substituents shift νM–N towards higher frequencies. This effect may be observed from the data in Fig. 30 where the complexes are arranged in order of decreasing values of F (i.e., increasing electron withdrawing capacity of X).

Quite apart from their secondary effect on the R-substituents, the electronic effects of X may directly transfer electron density to or from the M–N bonds. In an earlier study [64] of N-arylsalicylaldimine complexes with R = R' = H, only this direct mechanism was possible and νM–N was observed to shift to higher frequencies in relation to the Hammett substituent parameter, σ_p, which comprises both inductive and resonance contributions. The fact that the inductive effects of the X-substituents assume increased significance in the complexes with R-substituents suggests that in these complexes, the secondary effect of X on the electron releasing capacities of the R-substituents plays an important role in determining the M–N bond order and hence the value of νM–N. The difference between the relative significance of the inductive and mesomeric effects of the X-substituents in the salicylaldimine complexes with and without R-substituents illustrates the generalization [66] that there are not just two or three levels for the relative importance of field vs. resonance parameters but rather, a broad continuum, the precise balance between the two effects depending on both the molecular composition and the physical property being determined.

ACKNOWLEDGEMENTS

REFERENCES

1 H. Irving and R.J.P. Williams, J. Chem. Soc., (1953) 3192.
2 L. Sacconi and A. Sabatini, Nature, 186 (1960) 549.
3 L. Sacconi and A. Sabatini, J. Inorg. Nucl. Chem., 25 (1963) 1389.
4 R.W. Adams, R.L. Martin and G. Winter, Aust. J. Chem., 20 (1967) 773.
5 A.T. Hutton and D.A. Thornton, J. Mol. Struct., 39 (1977) 33.
6 L.G. Hulett and D.A. Thornton, Spectrochim. Acta, Part A, 27 (1971) 2089.

7   L.G. Hulett and D.A. Thornton, J. Mol. Struct., 13 (1972) 115.
8   L.G. Hulett and D.A. Thornton, Chimia, 26 (1972) 72.
9   L.G. Hulett and D.A. Thornton, Spectrosc. Lett., 5 (1972) 323.
10 L.G. Hulett and D.A. Thornton, Spectrochim. Acta, Part A, 29 (1973) 757.
11 L.G. Hulett and D.A. Thornton, J. Inorg. Nucl. Chem., 35 (1973) 2661.
12 H. Junge, Spectrochim. Acta, Part A, 24 (1968) 1957.
13 J.M. Robertson, J. Chem. Soc., (1951) 1222.
14 W.M. Macintyre, J.M. Robertson and R.F. Zahrobsky, Proc. R. Soc. London, Ser. A, 289 (1966) 161.
15 T.S. Davis, J.P. Fackler and M.J. Weeks, Inorg. Chem., 7 (1968) 1994.
16 A. Forman and L.E. Orgel, Mol. Phys., 2 (1959) 362.
17 R.D. Hancock and D.A. Thornton, J. Mol. Struct., 4 (1969) 361.
18 G.C. Percy and D.A. Thornton, Spectrosc. Lett., 3 (1970) 323.
19 R.D. Hancock and D.A. Thornton, Inorg. Nucl. Chem. Lett., 3 (1967) 419.
20 R.D. Hancock and D.A. Thornton, Inorg. Nucl. Chem. Lett., 3 (1967) 423.
21 R.D. Hancock and D.A. Thornton, J. Mol. Struct., 4 (1969) 377.
22 R.D. Hancock and D.A. Thornton, Theor. Chim. Acta, 19 (1970) 67.
23 G.S. Shephard and D.A. Thornton, Helv. Chim. Acta, 54 (1971) 2212.
24 C.A. Fleming and D.A. Thornton, J. Mol. Struct., 17 (1973) 79.
25 J.M. Haigh, N.P. Slabbert and D.A. Thornton, J. Inorg. Nucl. Chem., 32 (1970) 3635.
26 J.M. Haigh, N.P. Slabbert and D.A. Thornton, J. Mol. Struct., 7 (1971) 199.
27 G.C. Percy and D.A. Thornton, J. Inorg. Nucl. Chem., 35 (1973) 2719.
28 G.C. Percy and D.A. Thornton, Inorg. Nucl. Chem. Lett., 7 (1971) 599.
29 G.C. Percy and D.A. Thornton, J. Inorg. Nucl. Chem., 34 (1972) 3357.
30 G.C. Percy and D.A. Thornton, J. Inorg. Nucl. Chem., 34 (1972) 3369.
31 G.C. Percy and D.A. Thornton, J. Inorg. Nucl. Chem., 35 (1973) 2319.
32 G.S. Shephard and D.A. Thornton, J. Mol. Struct., 16 (1973) 321.
33 R.D. Hancock and D.A. Thornton, J. Mol. Struct., 6 (1970) 441.
34 J.M. Haigh, R.D. Hancock, L.G. Hulett and D.A. Thornton, J. Mol. Struct., 4 (1969) 369.
35 G.C. Percy and D.A. Thornton, J. Mol. Struct., 10 (1971) 39.
36 G. Anderegg, Helv. Chim. Acta, 46 (1963) 2397, 2813.
37 M.V. Veidis, G.H. Schreiber, T.E. Gough and G.J. Palenik, J. Am. Chem. Soc., 91 (1969) 1859.
38 B.W. Low, F.L. Hirshfeld and F.M. Richards, J. Am. Chem. Soc., 81 (1959) 4412.
39 P. George, D.S. McClure, J.S. Griffith and L.E. Orgel, J. Chem. Phys., 24 (1956) 1269.
40 T.L. Campbell and T. Moeller, J. Inorg. Nucl. Chem., 31 (1969) 1077.
41 T.L. Campbell and T. Moeller, J. Inorg. Nucl. Chem., 31 (1970) 945.
42 K.B. Yatsimirskii and N.A. Kostromina, Zh. Neorg. Khim., 9 (1964) 1793.
43 L.A.K. Staveley, D.R. Markham and M.R. Jones, J. Inorg. Nucl. Chem., 30 (1968) 231.
44 E.L. Muetterties and C.M. Wright, J. Am. Chem. Soc., 87 (1965) 4706.
45 G.S. Shephard and D.A. Thornton, J. Mol. Struct., 34 (1976) 83.
46 V.V. Zelentsov and V.K. Trunov, J. Struct. Chem. USSR, 2 (1961) 688.
47 M.A. Porai-Koshits and P.M. Zorkii, J. Struct. Chem. USSR, 2 (1961) 15.
48 D.H. Curtiss, F.K.C. Lyle and E.C. Lingafelter, Acta Crystallogr., 5 (1952) 388.
49 F.K.C. Lyle, B. Morosin and E.C. Lingafelter, Acta Crystallogr., 12 (1959) 938.
50 D.P. Graddon and G.M. Mockler, Aust. J. Chem., 20 (1967) 21; 21 (1968) 617, 907, 1487.
51 R.H. Holm and M.J. O'Connor, Prog. Inorg. Chem., 14 (1971) 241.
52 J.R. Miller and A.G. Sharpe, J. Chem. Soc., (1961) 2594.
53 J.A. Bevan, D.P. Graddon and J.F. McConnell, Nature (London), 199 (1969) 373.

54 A.J. McKinnon, T.N. Waters and D. Hall, J. Chem. Soc., (1964) 3290; (1965) 425.
55 L.E. Maley and D.P. Mellor, Nature (London), 161 (1948) 436; Aust. J. Sci. Res. Ser. A, 2 (1949) 92.
56 B.N. Figgis, Introduction to Ligand Fields, Interscience, New York, 1966, p. 244.
57 R.W. Taft, in M.S. Newman (Ed.), Steric Effects in Organic Chemistry, Wiley, New York, 1956, p. 591.
58 V.V. Zelentsov, P.M. Zorkii and M.A. Porai-Koshits, J. Struct. Chem. USSR, 4 (1963) 414.
59 J.M. Stewart, E.C. Lingafelter and J.D. Breazeale, Acta Crystallogr., 14 (1961) 888.
60 R.J.H. Clark and C.S. Williams, Inorg. Chem., 4 (1965) 350.
61 L.G. Hulett and D.A. Thornton, Spectrosc. Lett., 5 (1972) 323.
62 J.M. Haigh and D.A. Thornton, J. Mol. Struct., 8 (1971) 351.
63 R.H. Holm and G.W. Everett, Prog. Inorg. Chem., 7 (1966) 83.
64 G.C. Percy and D.A. Thornton, J. Inorg. Nucl. Chem., 35 (1973) 2319.
65 R.W. Taft, in M.S. Newman (Ed.), Steric Effects in Organic Chemistry, Wiley, New York, 1956, p. 591.
66 C.G. Swain and E.C. Lupton, J. Am. Chem. Soc., 90 (1968) 4328.